Chapter 3

Partitioned Element Methods

This chapter defines a general class of polytopal element formulations referred to as partitioned element methods (PEM). The essential characteristics and mathematical requirements placed upon these methods are formally stated, giving rise to a family of different approaches, for which some formal investigations are conducted in subsequent chapters. Several specific formulations are summarized in detail, and a number of existing methods are herein classified as particular instances of partitioned element methods.

3.1 Overview

Partitioned element methods are finite element-like methods which approach the task of constructing approximations to an arbitrary polytopal element's nodal shape functions by partitioning the element into sub-domains (quadrature cells). The element partition serves a dual purpose: it is used to establish a composite quadrature rule for the element, and to define a finite dimensional function space, from which the element's shape functions are selected as the solutions to corresponding boundary value problems, defined locally on the element.

Partitioned element methods are motivated by the idea that it is generally easier and more efficient to define complicated functions over arbitrary domains if the functions are defined in a piecewise polynomial fashion over simpler sub-domains. This is precisely the mentality which likewise motivates the finite element method and other related numerical approximation methods.

The PEM is driven by the need for establishing stable and efficient quadrature rules on arbitrary polytopes. Unlike virtual element methods which typically circumvent the use of quadrature altogether, partitioned element methods recognize the necessity of using domain quadrature rules to evaluate nonlinear residual and stiffness contributions. The use of sufficient quadrature also yields a stable integration of the weak form which does not rely upon unphysical stabilization parameters.

In contrast with traditional perspectives which regard the shape functions as being continuously defined on element domains (i.e. generalized barycentric coordinates), the PEM exploits the fact that the shape functions and their gradients only need to be evaluated at a discrete number of quadrature points. With this in mind, PEM approximation spaces are deliberately constructed around the quadrature cell partition of the element, and consequently resemble finite element approximation spaces.

The resulting approximations to the element's shape functions are altogether subject to the conditions of approximability, compatibility, stability, and quadrature consistency, as discussed in chapter 2. Together, these conditions impose a number of unique requirements upon the element's partition, it's corresponding quadrature rules, and the associated cell-based approximation spaces.

In the following sections, an abstract framework for the PEM is established, describing the shape function boundary value problems defined on an element, and their corresponding approximations. We further enumerate several specific partitioned element methods, and provide an assessment of their potential strengths and weaknesses.

3.2 Definition of Polytopal Element Shape Functions

Consider the structure of an arbitrary polyhedral element $\Omega \subset \mathbb{R}^3$, as depicted in Figure 3.1. The element's boundary $\partial\Omega$ may be subdivided into polygonal faces $F \subset \partial\Omega$, such that each face F is shared entirely with an adjacent element of the mesh, or with the mesh boundary. In turn, the boundary of each such face F may be subdivided into linear edges $E \subset \partial F$, such that each edge E is shared by one other face of the element. The end-points of each edge are called nodes, denoted V, and may be shared by multiple edges.

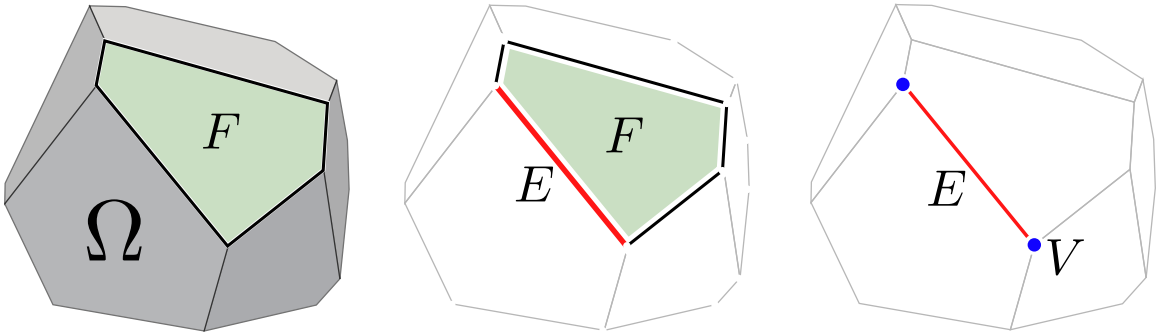

Figure 3.1: A representative polyhedral element $\Omega \subset \mathbb{R}^3$, a polygonal face $F \subset \partial\Omega$, a linear edge $E \subset \partial F$, and a node V.

The function spaces to which the element's shape functions belong are effectively broken Sobolev spaces, where a given shape function $\varphi \in \mathcal{W}_k(\overline{\Omega})$ is defined independently on the open interior of each polyhedral element $\Omega \subset \mathbb{R}^3$, and on its boundary $\partial\Omega$, such that

$$\mathcal{W}_k(\overline{\Omega}) = \left\{ \varphi|_\Omega \in H^k(\Omega) : \mathcal{L}_\Omega \varphi = f_\Omega \text{ in } \Omega,\ \varphi|_F \in \mathcal{W}_k(\overline{F})\ \forall F \in \partial\Omega \right\}, \tag{3.1}$$

$$\mathcal{W}_k(\overline{F}) = \left\{ \varphi|_F \in H^k(F) : \mathcal{L}_F \varphi = f_F \text{ in } F,\ \varphi|_E \in \mathcal{W}_k(\overline{E})\ \forall E \in \partial F \right\}, \tag{3.2}$$

$$\mathcal{W}_k(\overline{E}) = \left\{ \varphi|_E \in H^k(E) : \mathcal{L}_E \varphi = f_E \text{ in } E,\ \varphi|_V \in \mathbb{R}\ \forall V \in \partial E \right\}. \tag{3.3}$$

In essence, a given function $\varphi|_\Omega \in H^k(\Omega)$ defined on the element's interior is related to a corresponding boundary function $\varphi|_{\partial\Omega} \equiv \bar{\varphi}$ (which itself is a broken $H^k(\partial\Omega)$ function) via a well-posed Dirichlet boundary value problem:

$$\mathcal{L}_\Omega \varphi = f_\Omega \quad \forall \mathbf{X} \in \Omega \quad \text{s.t.} \quad \varphi = \bar{\varphi} \quad \forall \mathbf{X} \in \partial\Omega, \tag{3.4}$$

where $\mathcal{L}_\Omega$ denotes a linear differential operator, and $f_\Omega \in L^2(\Omega)$ is a generic forcing function. The element's degrees of freedom are collectively accounted for in the boundary function $\bar{\varphi}$, and in the forcing function f_Ω. Consequently, the interior function $\varphi|_\Omega$ is uniquely defined, provided there exists a unique solution to (3.4). In turn, we suppose that $\varphi|_F \in H^k(F)$ is the solution to a similar (2-dimensional) boundary value problem defined on each face F, and $\varphi|_E \in H^k(E)$ is the solution to a (1-dimensional) BVP on each edge E.

The advantage of defining shape functions in this manner is that it affords a great deal of flexibility in the construction of arbitrary order interpolants (or enhancement

functions), while maintaining $C^0(\mathcal{B}_0)$ continuity at inter-element interfaces. Moreover, given that the shape functions are uniquely defined at every point $\mathbf{X} \in \Omega$, they can be made amenable to post-processing and visualization-related tasks, if so desired.

Harmonic Shape Functions

The simplest choice of $\mathcal{L}_\Omega = -\nabla^2$ and $f_\Omega = 0$ corresponds to Laplace's equation:

$$\nabla^2 \varphi = 0 \quad \forall \mathbf{X} \in \Omega \quad \text{s.t.} \quad \varphi = \bar{\varphi} \quad \forall \mathbf{X} \in \partial\Omega, \tag{3.5}$$

whose solution φ is harmonic on Ω (and likewise on each face F and edge E – refer to Figure 3.2). Harmonic shape functions form a partition of unity, satisfy linear completeness, and arise from degrees of freedom borne only by the nodes of each element (i.e. the nodal values $\varphi|_V$); therefore, they satisfy the kronecker delta property. As such, harmonic shape functions constitute a class of generalized barycentric coordinates.

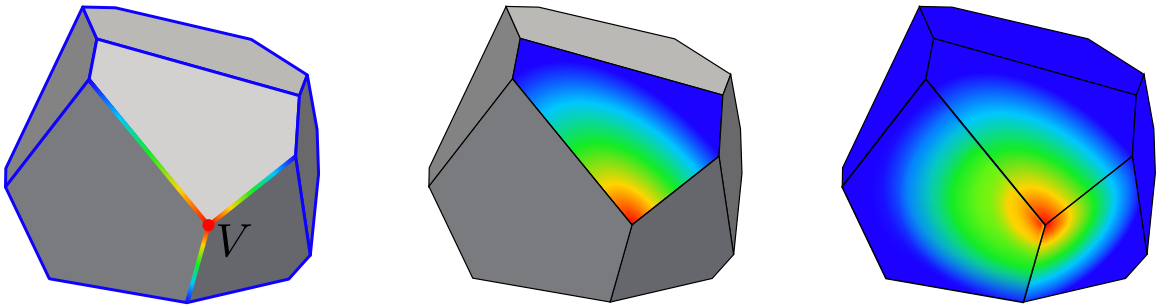

Figure 3.2: The harmonic shape function corresponding to the indicated node V, defined hierarchially on each edge, face, and the element.

If instead $f_\Omega \neq 0$ (corresponding to Poisson's equation), then

$$-\nabla^2 \varphi = f_\Omega \quad \forall \mathbf{X} \in \Omega \quad \text{s.t.} \quad \varphi = \bar{\varphi} \quad \forall \mathbf{X} \in \partial\Omega, \tag{3.6}$$

and we may introduce additional degrees of freedom through f_Ω belonging to the element (or its edges, faces). These degrees of freedom are effectively equivalent to bubble/enrichment functions; they are not directly associated with nodal evaluations of φ, but may be designed to exhibit certain desirable characteristics (e.g. to recover a particular order of polynomial completeness). The corresponding solution to (3.6) is not harmonic; instead, we shall refer to functions which satisfy (3.6) as *generalized harmonic shape functions*.

Harmonic shape functions are not a new concept; Gordon and Wixom were among the first authors to propose the idea in [27], and Martin et al. later considered their application to polyhedral finite elements in [37]. However, obtaining exact solutions to (3.5) is generally infeasible for arbitrary polyhedra. In practice, approximate solutions must be considered.

In particular, Bishop has proposed a method for constructing FE approximations to harmonic shape functions in [7]. Additionally, the VETFEM ([43], [45]) and the original PEM presented in [44], may be viewed as techniques for obtaining discrete approximations to harmonic shape functions. Likewise, many virtual element methods ([10], [15], [16]) suppose that the element shape functions are harmonic over individual element domains, though they are never explicitly constructed or represented as such.

It herein becomes of interest to determine suitable approximations to harmonic shape functions on arbitrary polyhedra. A number of methods to achieve this end are subsequently discussed.

3.3 Shape Function Approximation Methods

The exact solution $\varphi \in \mathcal{U}(\Omega) = \{\varphi \in H^1(\Omega) : \varphi = \bar{\varphi}\, \forall \mathbf{X} \in \partial\Omega\}$ to Poisson's equation in (3.6) (or Laplace's equation in (3.5) when $f_\Omega \equiv 0$) also satisfies the equivalent weak form:

$$\int_\Omega (\nabla^2 \varphi + f_\Omega)\eta \, dV = 0 \quad \forall \eta \in \mathcal{U}_0(\Omega), \tag{3.7}$$

or

$$\int_\Omega \nabla\varphi \cdot \nabla\eta \, dV = \int_\Omega f_\Omega \, \eta \, dV \quad \forall \eta \in \mathcal{U}_0(\Omega), \tag{3.8}$$

where $\mathcal{U}_0(\Omega) = \{\eta \in H^1(\Omega) : \eta = 0\, \forall \mathbf{X} \in \partial\Omega\}$ denotes an appropriately defined space of admissible variations – test functions.

A vast array of different variational methods may be employed to obtain an approximate solution $\varphi^h \in \mathcal{U}^h(\Omega)$ satisfying

$$\int_\Omega \nabla\varphi^h \cdot \nabla\eta^h \, dV = \int_\Omega f_\Omega \, \eta^h \, dV \quad \forall \eta^h \in \mathcal{U}_0^h(\Omega), \tag{3.9}$$

where $\mathcal{U}^h(\Omega)$ and $\mathcal{U}_0^h(\Omega)$ are taken to be finite-dimensional approximation spaces. Consequently, it is of interest to determine the essential requirements placed upon a given

approximation φ^h for the purposes of evaluating weak form integrals.

Specifically, for a finite element approximation to the model problem given in (2.36), consider the evaluation of an element's local bilinear form $a_\Omega(\mathbf{u}, \mathbf{v})$, where $\mathbf{u} = \sum_{a=1}^N \varphi_a \mathbf{u}_a$ and $\mathbf{v} = \sum_{a=1}^N \varphi_a \mathbf{v}_a$ are written in terms of the element's shape functions $\{\varphi_a\}_{a=1}^N$. An approximate evaluation of $a_\Omega(\mathbf{u}, \mathbf{v})$ is obtained by making the substitution $a_\Omega(\mathbf{u}^h, \mathbf{v}^h)$, where $\mathbf{u}^h = \sum_{a=1}^N \varphi_a^h \mathbf{u}_a$ and $\mathbf{v}^h = \sum_{a=1}^N \varphi_a^h \mathbf{v}_a$ are instead represented in terms of the approximations $\left\{\varphi_a^h\right\}_{a=1}^N$ to the element's shape functions.

According to the virtual element decomposition proposed in [15], we may express a given function $\mathbf{u} = \Pi_k^\Omega \mathbf{u} + (\mathbf{u} - \Pi_k^\Omega \mathbf{u})$ in terms of a low-order polynomial part $(\Pi_k^\Omega \mathbf{u})$ (up to degree k) and a non-polynomial part $(\mathbf{u} - \Pi_k^\Omega \mathbf{u})$, where $\Pi_k^\Omega : L^2(\Omega) \mapsto P^k(\Omega)$ is a corresponding polynomial projection operator satisfying $a_\Omega(\Pi_k^\Omega \mathbf{u}, \mathbf{v} - \Pi_k^\Omega \mathbf{v}) = 0 \ \forall \mathbf{u}, \mathbf{v}$, and thus

$$a_\Omega(\mathbf{u}, \mathbf{v}) = a_\Omega(\Pi_k^\Omega \mathbf{u}, \Pi_k^\Omega \mathbf{v}) + a_\Omega(\mathbf{u} - \Pi_k^\Omega \mathbf{u}, \mathbf{v} - \Pi_k^\Omega \mathbf{v}). \tag{3.10}$$

The first term appearing in the right-hand side of (3.10) accounts for the consistency of the finite element approximation, whereas the second term provides stability. To maintain consistency, the first term must be computed exactly, to the extent that

$$a_\Omega(\Pi_k^\Omega \mathbf{u}, \Pi_k^\Omega \mathbf{v}) = a_\Omega(\Pi_k^\Omega \mathbf{u}^h, \Pi_k^\Omega \mathbf{v}^h), \tag{3.11}$$

yielding the $k-$consistency property:

$$a_\Omega(\Pi_k^\Omega \mathbf{u}^h, \mathbf{v}^h) = a_\Omega(\Pi_k^\Omega \mathbf{u}, \mathbf{v}) \quad \forall \mathbf{v} \in \mathcal{V}^h(\Omega). \tag{3.12}$$

However, the second term need only be sufficiently well-approximated by

$$a_\Omega(\mathbf{u} - \Pi_k^\Omega \mathbf{u}, \mathbf{v} - \Pi_k^\Omega \mathbf{v}) \approx a_\Omega(\mathbf{u}^h - \Pi_k^\Omega \mathbf{u}^h, \mathbf{v}^h - \Pi_k^\Omega \mathbf{v}^h), \tag{3.13}$$

to the extent that the correct order of convergence is maintained, and the inf-sup condition is altogether satisfied. In [15], this is characterized by the assertion that there exist two positive constants a_* and a^* which are independent of the chosen discretization, such that the following stability condition holds:

$$a_* a_\Omega(\mathbf{v}, \mathbf{v}) \leq a_\Omega(\mathbf{v}^h, \mathbf{v}^h) \leq a^* a_\Omega(\mathbf{v}, \mathbf{v}) \quad \forall \mathbf{v} \in \mathcal{V}^h(\Omega). \tag{3.14}$$

It is argued that these conditions are necessary and sufficient to guarantee convergence of the resulting method when the local approximations $\mathbf{u}^h$ and $\mathbf{v}^h$ are used in place of $\mathbf{u}$ and $\mathbf{v}$.

It should be remarked that the evaluation of $a_\Omega(\mathbf{u}, \mathbf{v})$ will be further approximated through the use of numerical quadrature on Ω, herein denoted as $a^h_\Omega(\mathbf{u}, \mathbf{v})$. Alternatively, the use of low-order quadrature rules may be viewed as an exact integration of corresponding low-order approximations to $\mathbf{u}$ and $\mathbf{v}$, i.e. $\exists\, \mathbf{u}^h, \mathbf{v}^h$ such that $a^h_\Omega(\mathbf{u}, \mathbf{v}) = a_\Omega(\mathbf{u}^h, \mathbf{v}^h)$. The use of a numerical quadrature scheme is therefore subject to the conditions previously described.

With the above considerations borne in mind, we propose a set of minimal requirements on the resulting approximations $\mathbf{u}^h$ and $\mathbf{v}^h$, and their corresponding integration via an appropriately defined quadrature rule:

(I) $a^h_\Omega(\Pi^\Omega_k \mathbf{u}^h, \mathbf{v}^h) = a_\Omega(\Pi^\Omega_k \mathbf{u}, \mathbf{v}) \quad \forall \mathbf{v} \in \mathcal{V}^h(\Omega).$

(II) $a_* a_\Omega(\mathbf{v}, \mathbf{v}) \leq a^h_\Omega(\mathbf{v}^h, \mathbf{v}^h) \leq a^* a_\Omega(\mathbf{v}, \mathbf{v}) \quad \forall \mathbf{v} \in \mathcal{V}^h(\Omega).$

An important distinction should be made with regard to the requirements placed upon a given variational method used to construct approximations φ^h to (generalized) harmonic shape functions φ: it is not strictly necessary for the approximations to converge to φ as the dimension of $\mathcal{U}^h(\Omega)$ is systematically increased. Provided the above conditions are met, convergence of the overarching finite element method is altogether achieved, even if relatively coarse/low-order approximations to the shape functions are utilized. Moreover, relaxing the requirements placed upon the approximations (particularly with regard to continuity) can have advantageous side-effects: the resulting finite element solution is made less sensitive to the choice of discretization, and issues pertaining to elements with non-convex or degenerate features can be partially ameliorated.

The above considerations have prompted an investigation into the use of (discontinuous) low-order polynomial approximations to harmonic shape functions. These approximations are discussed in the following section.

Non-conforming Galerkin Approximations to (Generalized) Harmonic Shape Functions

If the boundary conditions imposed upon a given shape function are relaxed to the extent that $\varphi^h \neq \bar{\varphi}$ on $\partial\Omega$, then clearly $\mathcal{U}^h(\Omega) \not\subset \mathcal{U}(\Omega)$, and one must resort to the use of non-conforming approximation methods to obtain suitable approximations φ^h. In such cases, the boundary conditions must be imposed in a weak sense, such that φ^h still yields satisfaction of conditions (I) and (II), as developed in the previous section.

A number of weak enforcement strategies for the Dirichlet boundary condition ($\varphi = \bar{\varphi}$ on $\partial\Omega$) are suggested in the following sections.

Weak Enforcement of Boundary Conditions via a Lagrange Multiplier Method

One approach to weakly enforce the boundary condition $\varphi = \bar{\varphi}$ on $\partial\Omega$ would be to consider a Lagrange multiplier method, wherein

$$\min_{\varphi,\,\lambda} \mathcal{L}(\varphi, \lambda), \tag{3.15}$$

$$\mathcal{L}(\varphi, \lambda) \equiv \frac{1}{2}\int_\Omega \nabla\varphi \cdot \nabla\varphi \, dV - \int_\Omega f_\Omega \, \varphi \, dV + \int_{\partial\Omega} [\varphi - \bar{\varphi}] \, \lambda \, dA, \tag{3.16}$$

involving the specification of a Lagrange multiplier field $\lambda \in \Lambda(\partial\Omega) = \{\lambda \in L^2(\partial\Omega)\}$, and it's corresponding discrete approximation $\lambda^h \in \Lambda^h(\partial\Omega) \subset \Lambda(\partial\Omega)$. Differentiation of the Lagrangian yields two sets of equations in terms of the approximations $\varphi^h \in \mathcal{U}^h(\Omega)$ and $\lambda^h \in \Lambda^h(\partial\Omega)$:

$$\int_\Omega \nabla\varphi^h \cdot \nabla\eta^h \, dV - \int_\Omega f_\Omega \eta^h \, dV + \int_{\partial\Omega} \lambda^h \eta^h \, dA = 0 \quad \forall \eta^h \in \mathcal{U}^h(\Omega), \tag{3.17}$$

$$\int_{\partial\Omega} (\varphi^h - \bar{\varphi}) \, \mu^h \, dA = 0 \quad \forall \mu^h \in \Lambda^h(\partial\Omega). \tag{3.18}$$

Suppose finite-dimensional bases are established for $\mathcal{U}^h(\Omega)$ and $\Lambda^h(\partial\Omega)$, i.e.

$$\varphi^h(\mathbf{X}) = \sum_{a=1}^{N} \psi_a(\mathbf{X})\varphi_a, \quad \lambda^h(\mathbf{X}) = \sum_{a=1}^{M} \chi_a(\mathbf{X})\lambda_a, \tag{3.19}$$

such that

$$\sum_{a=1}^{N} \left[\int_\Omega \nabla\psi_a \cdot \nabla\psi_b \, dV\right] \varphi_a + \sum_{c=1}^{M} \left[\int_{\partial\Omega} \psi_b \, \chi_c \, dA\right] \lambda_c = \int_{\partial\Omega} f_\Omega \, \psi_b \, dA \quad \forall b, \tag{3.20}$$

$$\sum_{b=1}^{N} \left[\int_{\partial\Omega} \chi_c \, \psi_b \, dA \right] \varphi_b = \int_{\partial\Omega} \bar{\varphi} \, \chi_c \, dA \quad \forall c. \tag{3.21}$$

Given an appropriate selection for the indicated bases, the determination of the unknowns (φ_a and λ_a) entails the solution of a saddle-point system of equations, written in matrix-vector format:

$$\begin{bmatrix} \mathbf{A} & \mathbf{B} \\ \mathbf{B}^T & \mathbf{0} \end{bmatrix} \begin{Bmatrix} \boldsymbol{\varphi} \\ \boldsymbol{\lambda} \end{Bmatrix} = \begin{Bmatrix} \mathbf{f} \\ \bar{\boldsymbol{\varphi}} \end{Bmatrix}, \tag{3.22}$$

where

$$A_{ab} = \int_{\Omega} \nabla\psi_a \cdot \nabla\psi_b \, dV, \quad B_{bc} = \int_{\partial\Omega} \psi_b \, \chi_c \, dA, \tag{3.23}$$

$$f_b = \int_{\partial\Omega} f_\Omega \, \psi_b \, dA, \quad \bar{\varphi}_c = \int_{\partial\Omega} \bar{\varphi} \, \chi_c \, dA. \tag{3.24}$$

The main advantage of this approach is that virtually any space of functions may be selected for $\mathcal{U}^h(\Omega)$, such that the resulting approximations $\varphi^h \in \mathcal{U}^h(\Omega)$ can be made less sensitive to degenerate geometric features of the element (namely, short edges).

Arguably the simplest (and most efficient) choice is $\mathcal{U}^h(\Omega) = P^m(\Omega)$ where $m \geq k$, resembling certain formulations of the VETFEM ([43], [45]), where the basis functions for the Lagrange multiplier field are Dirac delta functions $\chi_c(\mathbf{X}) = \delta(\mathbf{X} - \mathbf{X}_c)$ $\forall c = 1, \ldots, N_v$ associated with the individual nodes of the element. A potential shortcoming of this particular choice for χ_c is that the resulting shape functions may nonetheless possess sharp gradients in the vicinity of short element edges, leading to undesirable behavior – poor numerical conditioning of the element's local stiffness matrix.

Various other choices for the Lagrange multiplier basis are possible which may yield less spurious approximations (for instance $\Lambda^h(\partial\Omega) = P^m(\partial\Omega)$). However, careful attention must be paid to the selection of $\mathcal{U}^h(\Omega)$ and $\Lambda^h(\partial\Omega)$, as poorly chosen bases can lead to ill-posedness of the saddle-point problem. More sophisticated linear solution methodologies may be required in these cases.

Weak Enforcement of Boundary Conditions via Nitsche's Method

As a viable alternative to the Lagrange multiplier method presented in the previous section, one may instead consider using Nitsche's method (refer to [32]) as a means of

weakly enforcing the boundary conditions for a given shape function, i.e.

$$\int_\Omega \nabla\varphi^h \cdot \nabla\eta^h \, dV + \int_{\partial\Omega} \left[\epsilon \frac{\partial\varphi^h}{\partial N}\eta^h - \varphi^h \frac{\partial\eta^h}{\partial N} \right] dA + \frac{\alpha}{|\partial\Omega|^\beta} \int_{\partial\Omega} \varphi^h \eta^h \, dA$$
$$= \int_\Omega f_\Omega \, \eta^h \, dV + \epsilon \int_{\partial\Omega} \bar{\varphi} \frac{\partial\eta^h}{\partial N} \, dA + \frac{\alpha}{|\partial\Omega|^\beta} \int_{\partial\Omega} \bar{\varphi}\eta^h \, dA \quad \forall \eta^h \in \mathcal{U}^h(\Omega), \tag{3.25}$$

where $\alpha > 0$ is a stabilization parameter, $|\partial\Omega|$ denotes the surface area of $\partial\Omega$, and $\beta = (d-1)^{-1}$ for $\Omega \subset \mathbb{R}^d$, $d \geq 2$. The parameter ϵ is canonically set equal to either -1 (yielding symmetry of the corresponding bilinear form on φ^h and η^h) or $+1$ (yielding coercivity).

Provided the stabilization parameter α is specified appropriately, the Galerkin approximation φ^h can be obtained as the solution to a positive-definite system of equations: $\mathbf{A}\boldsymbol{\varphi} = \mathbf{f}$, where

$$A_{ab} = \int_\Omega \nabla\psi_a \cdot \nabla\psi_b \, dV + \int_{\partial\Omega} \left[\epsilon \frac{\partial\psi_a}{\partial N}\psi_b - \psi_a \frac{\partial\psi_b}{\partial N} \right] dA + \frac{\alpha}{|\partial\Omega|^\beta} \int_{\partial\Omega} \psi_a \, \psi_b \, dA, \tag{3.26}$$

$$f_b = \int_\Omega f_\Omega \, \psi_b \, dV + \epsilon \int_{\partial\Omega} \bar{\varphi} \frac{\partial\psi_b}{\partial N} \, dA + \frac{\alpha}{|\partial\Omega|^\beta} \int_{\partial\Omega} \bar{\varphi} \, \psi_b \, dA. \tag{3.27}$$

As discussed in the previous section, a rather natural choice for the space of approximating functions is $\mathcal{U}^h(\Omega) = P^m(\Omega)$ with $m \geq k$. The resulting method yields reasonably well-conditioned stiffness matricies for convex shapes, even when the elements possess degenerate edges. However, experimental evidence suggests that for non-convex shapes, the resulting shape function approximations may succumb to Runge's phenomenon, yielding highly oscillatory approximations. A more thorough investigation of this behavior is presented in chapter 5.

These observations have led to the conclusion that approximations consisting of piecewise polynomials may yield more well-behaved (less oscillatory) solutions for φ^h. The remainder of our discussion will focus upon such methods.

3.4 Piecewise Polynomial Approximations to (Generalized) Harmonic Shape Functions

Partitioned element methods consider the approximation to a given element's shape functions via piecewise polynomials defined over a partition of the element's domain. In this

regard, the approach proposed by Bishop in [7] is properly regarded as a partitioned element method which utilizes C^0 FE approximations to harmonic shape functions. In like fashion, the eponymous partitioned element method introduced in [44] utilizes weakly continuous piecewise polynomial approximations to harmonic shape functions. Herein we propose a novel alternative approach based upon the interior penalty discontinuous Galerkin finite element method (henceforth, the DG-PEM).

A few preliminary definitions regarding the element's partition are given, followed by a more thorough discussion of several partition-based approximation methods.

The Element Partition

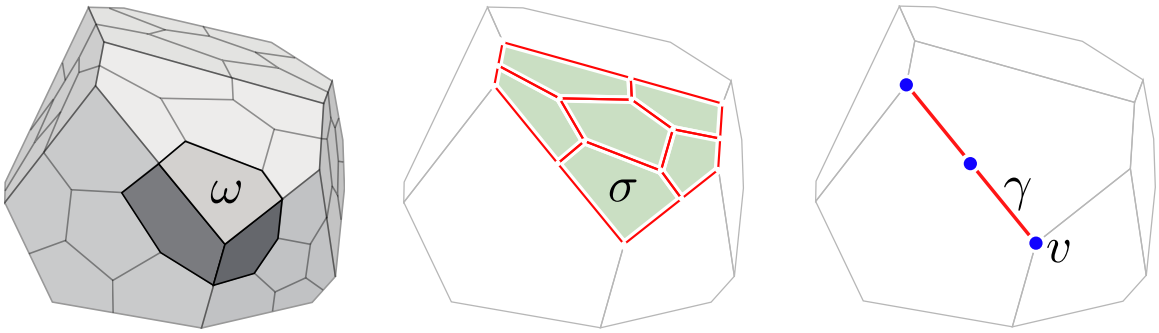

Figure 3.3: A representative polyhedral element $\Omega \subset \mathbb{R}^3$, and it's hierarchial partition into cells, facets, segments, and verticies.

Consider a partition $\mathcal{T}_\omega(\Omega)$ of a given polyhedral element Ω into polyhedral cells $\omega \subset \Omega$. The boundary of each cell consists of polygonal facets $\sigma \subset \partial\omega$. Further, denote by Γ_ω the set of all interior cell interfaces (facets) shared by two adjacent cells, such that a given polygonal facet σ belongs either to Γ_ω, or to the boundary of the element $\partial\Omega$.

In turn, let $\mathcal{T}_\sigma(F)$ denote the partition of a given face $F \subset \partial\Omega$ into polygonal facets $\sigma \subset F$. The boundary of each facet consists of linear segments $\gamma \subset \partial\sigma$. For a given face F, let Γ_σ denote the set of all interior facet interfaces (segments) shared by two facets belonging to F, such that a given linear segment γ belongs either to Γ_σ or ∂F.

Finally, $\mathcal{T}_\gamma(E)$ denotes the partition of a given edge $E \subset \partial F$ into linear segments $\gamma \subset E$. The endpoints of each segment are called verticies, denoted v. For a given edge E, denote by Γ_γ the set of all interior segment interfaces (verticies) shared by two segments belonging to E, such that a given vertex v belongs either to Γ_γ or ∂E. As well,

each node V corresponds to a single vertex v, though not all verticies coincide a node.

A number of simple partitioning schemes (as illustrated in Figure 3.4) are proposed:

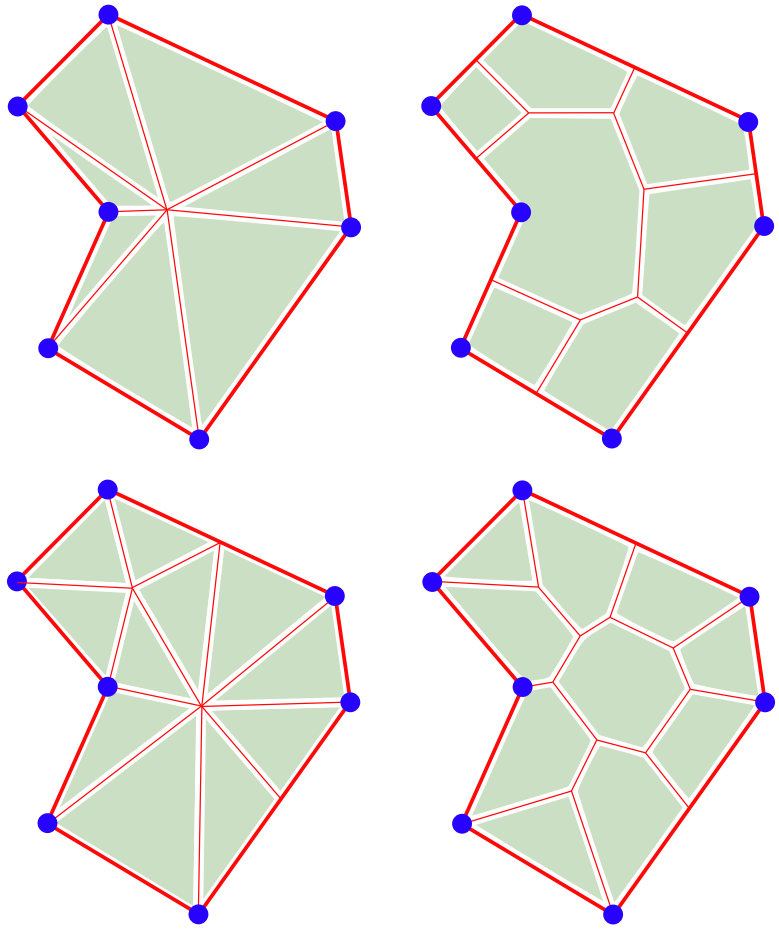

Figure 3.4: Polygonal element partitioning schemes: (top-left) edge-based partition, (top-right) node-based partition, (bottom-left) random Delaunay partition, (bottom-right) random Voronoi partition.

- **Edge-based**: For star-convex shapes – the vertex-averaged centroid is used to subdivide the element into triangles (in 2D) or tetrahedra (in 3D) and associated with each linear edge of the element.

- **Node-based**: For arbitrary shapes – the element is sub-divided into quadrature cells corresponding to the tributary area surrounding each node.

- **Random Delaunay**: For arbitrary shapes – the element is sub-divided into a Delaunay triangulation (in 2D) or tetrahedralization (in 3D), whose corresponding

verticies are generated via a random point sampling process.

- **Random Voronoi**: For arbitrary shapes – the element is sub-divided into Voronoi cells, whose corresponding voronoi sites are generated via a constrained maximal poisson-disk sampling process, as described in [20].

We denote the volume of a given cell as $|\omega|$, the area of a facet as $|\sigma|$, and the length of a segment as $|\gamma|$. Each facet likewise possesses an associated normal direction $\mathbf{N}_\sigma$, whose orientation is outward from Ω for all $\sigma \in \partial\Omega$. The orientation of $\mathbf{N}_\sigma$ is otherwise arbitrary for all $\sigma \in \Gamma_\omega$ (for a given facet σ shared by two cells ω_1 and ω_2, $\mathbf{N}_\sigma$ may be defined as being outward with respect to either ω_1 or ω_2.)

Continuous Galerkin Approximations to (Generalized) Harmonic Shape Functions

Consider finite dimensional sub-spaces $\mathcal{U}^h(\Omega) \subset \mathcal{U}(\Omega)$ and $\mathcal{U}_0^h(\Omega) \subset \mathcal{U}_0(\Omega)$. The Galerkin approximation $\varphi^h \in \mathcal{U}^h(\Omega)$ to a given (generalized) harmonic shape function $\varphi \in \mathcal{U}(\Omega)$ satisfies

$$\int_\Omega \nabla\varphi^h \cdot \nabla\eta^h \, dV = \int_\Omega f_\Omega \, \eta^h \, dV \quad \forall \eta^h \in \mathcal{U}_0^h(\Omega). \tag{3.28}$$

Bishop has already explored such an approach in [7] for constructing approximations to harmonic shape functions using a partition of a given polyheral element into sub-dividing tetrahedra. The approximation space $\mathcal{U}^h(\Omega)$ is spanned by the $C^0(\Omega)$ finite element basis functions defined on the tetrahedral partition of Ω. The corresponding shape function approximations $\varphi^h \in \mathcal{U}^h(\Omega)$ are obtained as the solutions to a set of local finite element problems defined on Ω (and its faces, edges – refer to Figure 3.5).

It was demonstrated that the resulting approximations φ^h preserve low-order polynomial completeness – a consequence of $\mathcal{U}^h(\Omega) \supset P^1(\Omega)$. If the elements are discretized into a sufficient number of tetrahedra, the method is observed to be both stable and consistent (provided a supplementary gradient correction scheme is employed to account for the effects of integration error).

For coarse tetrahedral sub-divisions, the local FE problems that must be solved on each element are relatively small, in some cases entailing only a single degree of freedom

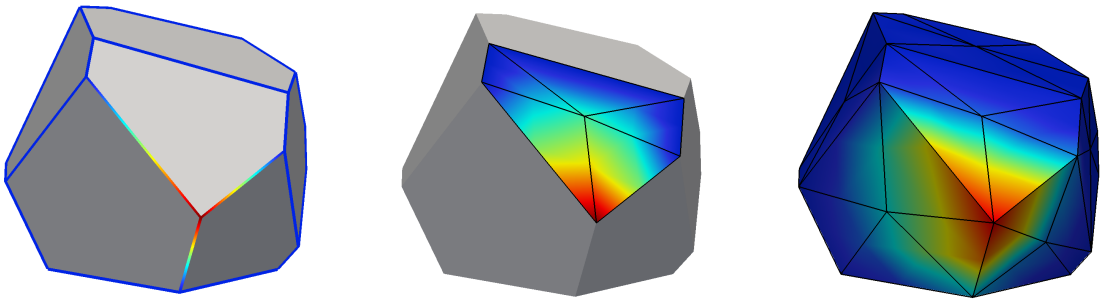

Figure 3.5: The FE-PEM approximation to a given harmonic shape function, defined hierarchially on the element's faces and edges.

(assocaited with an interior vertex) that must be solved for. Otherwise, the approach can become computationally expensive if the elements are subdivided into an excessively large number of tetrahedra (in the event that more accurate/refined approximations to the shape functions are desired). However, initial numerical investigations have suggested that relatively coarse tetrahedral sub-divisions of the elements provide sufficiently accurate results; further subdivision (tetrahedral $h-$refinement) does little to improve the overall accuracy of the method.

A natural extension of the method to higher-order serendipity elements would be to consider $p-$refinement of an element's tetrahedral subdivision to recover higher-order polynomial completeness, i.e. to guarantee $\mathcal{U}^h(\Omega) \supset P^k(\Omega)$ for some desired polynomial order k. However, the construction of shape functions on a given element would likely bear a much higher computational cost with increasing polynomial degree, owing to the increased size of the local FE problems on Ω. Moreover, the specification of stable and accurate numerical quadratures would present an additional challenge.

A separate generalization would be to consider subdividing the elements into arbitrary polyhedra, and solving (3.28) by means of the virtual element method. This would allow for a more natural collocation of quadrature cells with the specified subdivision, resembling the partitioned element method proposed in [44].

As will be discussed in chapter 5, a particular complication arises for harmonic shape functions and their corresponding $C^0(\Omega)$ approximations on irregularly shaped elements: the solution to Laplace's equation may possess extremely sharp gradients if the geometry

of the element contains reflex corners or nearly degenerate features (i.e. short edges). A consequence of this is poor conditioning of the element's local stiffness matrix, leading to excessively stiff modes of deformation (locking), and issues of numerical conditioning in the linear solution process.

As discussed previously, it becomes of interest to consider non-conforming approximations $\varphi^h \in \mathcal{U}^h(\Omega) \not\subset \mathcal{U}(\Omega)$ which have the potential to overcome these issues. A particular solution is henceforth explored in the form of discontinuous Galerkin finite element approximations to harmonic shape functions.

Discontinuous Galerkin Approximations to (Generalized) Harmonic Shape Functions

Consider the broken Sobolev space $\mathcal{D}_k^h(\Omega) = \left\{\varphi \in L^2(\Omega) : \varphi|_\omega \in P^k(\omega)\, \forall \omega \in \mathcal{T}_\omega(\Omega)\right\}$ consisting of (discontinuous) piecewise polynomials defined over the partition of the element. The interior penalty discontinuous Galerkin method described in [47] is applied to (3.8) to obtain approximations $\varphi^h \in \mathcal{D}_k^h(\Omega) \not\subset \mathcal{U}(\Omega)$ to generalized harmonic shape functions $\varphi \in \mathcal{U}(\Omega)$, satisfying

$$\sum_{\omega\in\mathcal{T}_\omega(\Omega)} \int_\omega \nabla\varphi^h \cdot \nabla\eta^h \, dV + \sum_{\sigma\in\Gamma_\omega\cup\partial\Omega} \int_\sigma \left(\epsilon \left\{ \frac{\partial\varphi^h}{\partial N_\sigma} \right\} [\![\eta^h]\!] - [\![\varphi^h]\!] \left\{ \frac{\partial\eta^h}{\partial N_\sigma} \right\} \right) dA$$
$$+ J_0(\varphi^h, \eta^h) + J_1(\varphi^h, \eta^h) = \int_\Omega f_\Omega \, \eta^h \, dV + \sum_{\sigma\in\partial\Omega} \int_\sigma \left(\frac{\alpha_{\sigma 0}}{|\sigma|^{\beta_0}} \eta^h + \epsilon \frac{\partial\eta^h}{\partial N_\sigma} \right) \bar{\varphi} \, dA \qquad (3.29)$$

for all $\eta^h \in \mathcal{D}_k^h(\Omega)$, where

$$\{\varphi\} = \frac{1}{2}(\varphi|_{\omega_1} + \varphi|_{\omega_2}), \quad [\![\varphi]\!] = (\varphi|_{\omega_1} - \varphi|_{\omega_2}) \quad \forall \sigma = \partial\omega_1 \cap \partial\omega_2, \qquad (3.30)$$

$$\{\varphi\} = [\![\varphi]\!] = \varphi|_\omega \quad \forall \sigma = \partial\omega \cap \partial\Omega, \qquad (3.31)$$

and where

$$J_0(\varphi^h, \eta^h) = \sum_{\sigma\in\Gamma_\omega\cup\partial\Omega} \frac{\alpha_{\sigma 0}}{|\sigma|^{\beta_0}} \int_\sigma [\![\varphi^h]\!] \, [\![\eta^h]\!] \, dA, \qquad (3.32)$$

$$J_1(\varphi^h, \eta^h) = \sum_{\sigma\in\Gamma_\omega} \frac{\alpha_{\sigma 1}}{|\sigma|^{\beta_1}} \int_\sigma \left[\!\!\left[\frac{\partial\varphi^h}{\partial N_\sigma} \right]\!\!\right] \left[\!\!\left[\frac{\partial\eta^h}{\partial N_\sigma} \right]\!\!\right] dA. \qquad (3.33)$$

$J_0(\varphi^h, \eta^h)$ and $J_1(\varphi^h, \eta^h)$ are supplementary bilinear forms which penalize jumps in the indicated functions' values and their normal derivatives at cell boundaries. The parameters $\alpha_{\sigma 0}$, β_0, must be appropriately specified such that $\alpha_{\sigma 0} > 0$ is sufficiently large, and $\beta_0(d-1) \geq 1$ where $\Omega \subset \mathbb{R}^d$, $d \geq 2$; the specification of $\alpha_{\sigma 1}$, β_1 is less strict, allowing for $\alpha_{\sigma 1} \geq 0 \ \forall \sigma$. The parameter $\epsilon \in \{-1, 0, +1\}$ determines which interior penalty method is employed:

$\epsilon = -1$: The symmetric interior penalty Galerkin (SIPG) method.

$\epsilon = 0$: The incomplete interior penalty Galerkin (IIPG) method.

$\epsilon = +1$: The nonsymmetric interior penalty Galerkin (NIPG) method.

As a matter of terminology, the above methods will henceforth collectively be referred to by the acronym DG-PEM (discontinuous Galerkin partitioned element methods).

If one considers a non-dimensional analysis where $\mathbf{X} = h_\Omega \mathbf{X}'$, and h_Ω denotes a characteristic length scale corresponding to the diameter of the element Ω, the following quantities may be expressed in terms of their non-dimensional counterparts:

$$dV = h_\Omega^d dV', \quad dA = h_\Omega^{d-1} dA', \quad \nabla = h_\Omega^{-1} \nabla', \quad |\sigma| = h_\Omega^{d-1} |\sigma'|, \quad f_\Omega = h_\Omega^{-2} f_{\Omega'}. \tag{3.34}$$

It is presumed that $\alpha_{\sigma 0}$, $\alpha_{\sigma 1}$ are defined independently of h_Ω. Consequently,

$$\begin{aligned}
&h_\Omega^{d-2} \left[\sum_{\omega' \in \mathcal{T}_{\omega'}(\Omega')} \int_{\omega'} \nabla' \varphi^h \cdot \nabla' \eta^h \, dV' - \int_{\Omega'} f_{\Omega'} \, \eta^h \, dV' - \sum_{\sigma' \in \partial \Omega'} \int_{\sigma'} \epsilon \frac{\partial \eta^h}{\partial N_{\sigma'}} \, \bar{\varphi} \, dA' \right. \\
&\qquad \left. + \sum_{\sigma' \in \Gamma_{\omega'} \cup \partial \Omega'} \int_{\sigma'} \left(\epsilon \left\{ \frac{\partial \varphi^h}{\partial N_{\sigma'}} \right\} [\![\eta^h]\!] - [\![\varphi^h]\!] \left\{ \frac{\partial \eta^h}{\partial N_{\sigma'}} \right\} \right) dA' \right] \\
&+ h_\Omega^{(d-1)(1-\beta_0)} \left[\sum_{\sigma' \in \Gamma_{\omega'} \cup \partial \Omega'} \frac{\alpha_{\sigma 0}}{|\sigma'|^{\beta_0}} \int_{\sigma'} [\![\varphi^h]\!] \, [\![\eta^h]\!] \, dA' - \sum_{\sigma' \in \partial \Omega'} \frac{\alpha_{\sigma 0}}{|\sigma'|^{\beta_0}} \int_{\sigma'} \eta^h \, \bar{\varphi} \, dA' \right] \\
&+ h_\Omega^{(d-1)(1-\beta_1)-2} \left[\sum_{\sigma' \in \Gamma_{\omega'}} \frac{\alpha_{\sigma 1}}{|\sigma'|^{\beta_1}} \int_{\sigma'} \left[\!\!\left[\frac{\partial \varphi^h}{\partial N_{\sigma'}} \right]\!\!\right] \left[\!\!\left[\frac{\partial \eta^h}{\partial N_{\sigma'}} \right]\!\!\right] dA' \right] = 0 \quad \forall \eta^h \in \mathcal{D}_k^h(\Omega).
\end{aligned} \tag{3.35}$$

To maintain dimensional consistency, it is suggested that β_0 and β_1 be chosen such that

$$\beta_0 = (d-1)^{-1}, \quad \beta_1 = -(d-1)^{-1}. \tag{3.36}$$

To ensure that the resulting linear system of equations is reasonably well-conditioned, the penalty parameters $\alpha_{\sigma 0}$, $\alpha_{\sigma 1}$ should not be made excessively large. Nonetheless, an interesting limiting case occurs when $\alpha_{\sigma 0}, \alpha_{\sigma 1} \to \infty$ proportionally:

$$J_0(\varphi^h, \eta^h) + J_1(\varphi^h, \eta^h) = \sum_{\sigma \in \partial\Omega} \frac{\alpha_{\sigma 0}}{|\sigma|^{\beta_0}} \int_\sigma \eta^h \, \bar{\varphi} \, dA \quad \forall \eta^h \in \mathcal{D}_k^h(\Omega). \tag{3.37}$$

The above is henceforth refered to as the *pure penalty* DG-PEM. Under certain conditions (for particular choices of $\mathcal{T}_\omega(\Omega)$ and $\mathcal{D}_k^h(\Omega)$), the pure penalty variant of the DG-PEM may in fact yield unique solutions φ^h which altogether satisfy conditions of consistency and stability detailed in section 3.3. However, the bilinear form arising from the penalty terms J_0 and J_1 alone is not guaranteed to be elliptic, in general. Additional (higher order flux) penalty terms may be necessary, i.e.

$$J_s(\varphi^h, \eta^h) = \sum_{\sigma \in \Gamma_\omega} \frac{\alpha_{\sigma s}}{|\sigma|^{\beta_s}} \int_\sigma \left[\!\left[\frac{\partial^s \varphi^h}{\partial N_\sigma^s} \right]\!\right] \left[\!\left[\frac{\partial^s \eta^h}{\partial N_\sigma^s} \right]\!\right] dA \tag{3.38}$$

for $s \leq k$, $\alpha_{sigmas} > 0$, and $\beta_s = (1 - 2s)/(d - 1)$. These may be used to supplement the stability of the pure penalty approach, particularly when $k > 1$.

The majority of our subsequent analyses will explore the family of 3-parameter methods arising from

$$\alpha_{\sigma 0} = \alpha_0|_{\partial\Omega} \; \forall \sigma \in \partial\Omega, \quad \alpha_{\sigma 0} = \alpha_0|_{\Gamma_\omega} \; \forall \sigma \in \Gamma_\omega, \quad \alpha_{\sigma 1} = \alpha_1|_{\Gamma_\omega} \; \forall \sigma \in \Gamma_\omega, \tag{3.39}$$

notably entailing a separate penalization of the boundary condition via $\alpha_0|_{\partial\Omega}$. Decreasing the value of $\alpha_0|_{\partial\Omega}$ is tantamount to relaxing the degree to which the boundary condition is enforced. The effects of this will be examined and discussed in chapter 5.

3.5 Partition-Based Quadrature Rules

If arbitrary polytopal shapes are to be used as elements in the PEM, then there arises a need for devising a means of integrating contributions to the weak form, ostensibly through the use of domain quadrature rules. Such rules must be sufficiently stable (utilizing a sufficient number of well-positioned quadrature points) and accurate (capable of exactly integrating low-order polynomials up to some specified degree).

Partitioned element methods approach this task by subdividing the elements (and their boundaries) into a sufficient number of polytopal sub-domains which are used as integration cells. For the sake of simplicity, the element's cell partition $\mathcal{T}_\omega(\Omega)$ (which is used to construct the element's shape functions) is collocated with the integration cells. Low-order (i.e. 1-point) quadrature rules are defined on each of these sub-domains, and a composite quadrature rule for the element is constructed from the set of all quadrature points defined in this manner. In general, such rules are straightforward to define, but will have limited accuracy. Consequently, appropriate modifications must be made to satisfy Galerkin exactness for certain low-order polynomial solutions.

Methods for partitioning the elements into sub-domains which yield stable and efficient composite quadrature rules are addressed in the following section. A discussion is given later on to the correction of these quadratures for the sake of satisfying Galerkin exactness (quadrature consistency).

Composite Quadrature Rules

Given a partition of an element into polytopal sub-domains (quadrature cells), one may utilize low order quadrature rules over each sub-domain, thereby yielding a composite quadrature rule over the element as a whole, whose overall accuracy is determined by the order of accuracy used within each sub-domain.

The simplest quadrature rule of this form is the composite mid-point scheme, where the quadrature points are located at the centroids of each sub-domain. Such a rule exactly integrates polynomials up to first order, and provides reasonable accuracy when integrating polynomials of higher-order ([44] provides a numerical assessment of the accuracy of composite mid-point quadratures.) Moreover, the integration points are guaranteed to be interior to each sub-domain (and the element as a whole), provided each cell is convex.

For simple sub-divisions (consisting of triangles or tetrahedra), composite quadrature rules may be extended rather naturally to obtain higher-order accuracy. For generic sub-divisions (consiting of arbitrary polytopes), the extension to higher-order composite rules is not as straight-forward. For this reason, subsequent discussions will be concerned almost exclusively with composite mid-point rules.

The weights and locations of a composite mid-point quadrature rule correspond to the volumes and geometric centroids of each cell. In general, a given quadrature cell ω may be an arbitrary polyhedron, whose volume $|\omega|$ and centroid $\bar{\mathbf{X}}$ may be computed using the 0-th and 1-st order moments of ω, i.e.

$$|\omega| = \int_\omega dV, \quad \bar{\mathbf{X}} = \frac{\int_\omega \mathbf{X}\, dV}{\int_\omega dV}. \tag{3.40}$$

Using the method proposed by Chin et al. in [12], the computation of monomial moments of arbitrary degree $|\alpha|$ may be effected via an integral over $\partial\omega$:

$$\int_\omega \mathbf{X}^\alpha\, dV = \frac{1}{d+|\alpha|} \int_{\partial\omega} (\mathbf{X}\cdot\mathbf{N})\, \mathbf{X}^\alpha\, dA, \tag{3.41}$$

for any arbitrary polytope $\omega \subset \mathbb{R}^d$. If $\partial\omega$ may be partitioned into a collection of $d-1$ dimensional facets $\sigma \subset \partial\omega$, then

$$\int_\omega \mathbf{X}^\alpha\, dV = \frac{1}{d+|\alpha|} \sum_{\sigma\in\partial\omega} \int_\sigma (\mathbf{X}\cdot\mathbf{N}_\sigma)\, \mathbf{X}^\alpha\, dA, \tag{3.42}$$

where $\mathbf{N}_\sigma$ is the outward (with respect to ω) unit normal associated with facet σ. We remark that any location $\mathbf{X}$ positioned on a given facet σ may be expressed as

$$\mathbf{X} = \mathbf{X}_\sigma + \sum_{i=1}^{d-1} X_i\, \hat{\mathbf{X}}_i, \tag{3.43}$$

where $\mathbf{X}_\sigma$ is any reference location positioned on the hyperplane which contains σ, and the orthonomial set $\left\{\hat{\mathbf{X}}_i\right\}_{i=1}^{d-1}$ defines a parameterization of the in-plane coordinates on σ. This leads to the observation $\mathbf{X}\cdot\mathbf{N}_\sigma = \mathbf{X}_\sigma\cdot\mathbf{N}_\sigma\ \forall\mathbf{X}\in\sigma$, and thus

$$\int_\omega \mathbf{X}^\alpha\, dV = \frac{1}{d+|\alpha|} \sum_{\sigma\in\partial\omega} (\mathbf{X}_\sigma\cdot\mathbf{N}_\sigma) \int_\sigma \mathbf{X}^\alpha\, dA. \tag{3.44}$$

The integral of $\mathbf{X}^\alpha$ over each facet may in turn be carried out via

$$\int_\sigma \mathbf{X}^\alpha\, dA = \frac{1}{d-1+|\alpha|} \left[\sum_{\gamma\in\partial\sigma} \left((\mathbf{X}_\gamma - \mathbf{X}_\sigma)\cdot\mathbf{N}_\gamma\right) \int_\gamma \mathbf{X}^\alpha\, dS + \mathbf{X}_\sigma \cdot \int_\sigma \nabla\mathbf{X}^\alpha\, dA \right], \tag{3.45}$$

and the integral over each segment is

$$\int_\gamma \mathbf{X}^\alpha\, dS = \frac{1}{d-2+|\alpha|} \left[\sum_{v\in\partial\gamma} \left((\mathbf{X}_v - \mathbf{X}_\gamma)\cdot\mathbf{N}_v\right)\mathbf{X}_v^\alpha + \mathbf{X}_\gamma \cdot \int_\gamma \nabla\mathbf{X}^\alpha\, dS \right]. \tag{3.46}$$

Similarly defined composite rules may be defined on each polygonal face of a given polyhedral element, or on each edge of a polygonal element. However, while composite mid-point quadrature rules are able to provide reasonable accuracy, they will not necessarily lead to quadrature consistency, as expressed in (2.67). For this reason, a gradient correction scheme (such as the one proposed by Bishop in [7], or by Talischi in [59]) must be employed, as discussed in the following section.

Gradient Correction Scheme

Consider an element $\Omega \subset \mathbb{R}^d$ upon which is specified a domain quadrature rule $\{\mathbf{X}_q,\, w_q\}_{q=1}^{N_{qp}}$ such that the integral of a scalar function $f \in L^2(\Omega)$ over Ω is approximated by

$$\int_\Omega f\, dV \approx \sum_{q=1}^{N_{qp}} w_q f(\mathbf{X}_q). \tag{3.47}$$

Additionally, suppose that each face $F \subset \partial\Omega$ possesses a quadrature rule $\left\{\mathbf{X}_b,\, w_b,\, \mathbf{N}^{(b)}\right\}_{b=1}^{N_{bp}^F}$ where $\mathbf{N}^{(b)}$ denotes the unit normal to the face F evaluated at $\mathbf{X}_b \in F$. The integral of a scalar function $f \in L^2(\partial\Omega)$ (or of a vector-valued function $f\,\mathbf{N}$) over $\partial\Omega$ is approximated by

$$\int_{\partial\Omega} f\, dA \approx \sum_{F\in\partial\Omega} \sum_{b=1}^{N_{bp}^F} w_b f(\mathbf{X}_b), \quad \int_{\partial\Omega} f\,\mathbf{N}\, dA \approx \sum_{F\in\partial\Omega} \sum_{b=1}^{N_{bp}^F} w_b f(\mathbf{X}_b)\mathbf{N}^{(b)}. \tag{3.48}$$

Suppose that the aforementioned quadrature rules (on a given polyhedral element Ω and on each of its polygonal faces $F \subset \partial\Omega$) are constructed using the composite mid-point quadrature scheme discussed in the previous section. A simple gradient correction scheme is obtained by introducing an auxiliary field $\boldsymbol{\xi} = \nabla\phi - \nabla\varphi$, such that a given trial function φ and its corresponding test function ϕ differ (minimally), to the extent that the quadrature consistency conditions hold:

$$\sum_{q=1}^{N_{qp}} w_q \left[\mathbf{X}_q^\alpha\, \nabla\phi(\mathbf{X}_q) + \nabla\mathbf{X}_q^\alpha\, \phi(\mathbf{X}_q)\right] = \sum_{F\in\partial\Omega} \sum_{b=1}^{N_{bp}^F} w_b \mathbf{X}_b^\alpha \phi(\mathbf{X}_b)\mathbf{N}^{(b)} \quad \forall |\alpha| \leq k-1, \tag{3.49}$$

for every test function ϕ, where k represents the degree of polynomial completeness exhibited by the space of trial solutions. Given the discrete conditions:

$$\phi(\mathbf{X}_b) = \varphi(\mathbf{X}_b)\,\forall b, \quad \phi(\mathbf{X}_q) = \varphi(\mathbf{X}_q)\,\forall q, \quad \nabla\phi(\mathbf{X}_q) = \nabla\varphi(\mathbf{X}_q) + \boldsymbol{\xi}(\mathbf{X}_q)\,\forall q, \tag{3.50}$$

we obtain $\boldsymbol{\xi}(\mathbf{X}_q)$ as the solution to the quadratic minimization problem:

$$\min_{\boldsymbol{\xi}} \frac{1}{2}||\boldsymbol{\xi}||_{\Omega}^2, \tag{3.51}$$

subject to (3.49), where $||\boldsymbol{\xi}||_{\Omega}$ is deliberately approximated using the element's quadrature rule, i.e.

$$||\boldsymbol{\xi}||_{\Omega} \approx \left[\sum_{q=1}^{N_{qp}} w_q \, [\xi_i(\mathbf{X}_q)\, \xi_i(\mathbf{X}_q)]\right]^{1/2}. \tag{3.52}$$

Suppose two adjacent elements Ω_L and Ω_R share a given face $F = \partial\Omega_L \cap \partial\Omega_R$. If the shape functions and quadrature rules defined on $F_L \subset \partial\Omega_L$ and $F_R \subset \partial\Omega_R$ (where $F_L = F_R$) are identical, then the aforementioned gradient correction scheme will automatically lead to satisfaction of finite element patch tests. However, if Ω_L and Ω_R provide separate quadrature rules on F_L and F_R (arising from different partitions of the shared face), or if the elements' shape functions are not defined identically on F_L and F_R, then we require that an additional condition be met:

$$\sum_{l=1}^{N_{bp}^{F_L}} w_l \mathbf{X}_l^{\alpha} \phi_l \, \mathbf{N}^{(l)} = -\sum_{r=1}^{N_{bp}^{F_R}} w_r \mathbf{X}_r^{\alpha} \phi_r \, \mathbf{N}^{(r)} \quad \forall \, |\alpha| \leq k-1, \tag{3.53}$$

for every shared face $\partial\Omega_L \subset F_L = F_R \subset \partial\Omega_R$.

As an alternative to using a gradient correction scheme, a novel approach to restore quadrature consistency (inspired by the virtual element method) is presented in the following section.

Selective Modal Quadrature

Consider all functions $f \in L^2(\Omega)$ represented over an arbitrary polytopal element domain $\Omega \subset \mathbb{R}^d$. Borrowing from notation typical of the VEM, consider an $L^2(\Omega)$ polynomial projection operator $\Pi_k^{\Omega} : L^2(\Omega) \mapsto P^k(\Omega)$ which may be used to decompose $f = f_p + f_n$ into polynomial and non-polynomial parts:

$$f_p = \Pi_k^{\Omega} f, \quad f_n = f - \Pi_k^{\Omega} f = \pi_k^{\Omega} f, \tag{3.54}$$

where $\pi_k^{\Omega} : L^2(\Omega) \mapsto L^2(\Omega) \backslash P^k(\Omega)$. Consequently, we observe that $\Pi_k^{\Omega} f$ is $L^2(\Omega)$ orthogonal to any $\pi_k^{\Omega} g$ for all $g \in L^2(\Omega)$, to the extent that

$$\int_{\Omega} (\Pi_k^{\Omega} f)(g - \Pi_k^{\Omega} g) \, dv = \langle \Pi_k^{\Omega} f, g - \Pi_k^{\Omega} g \rangle_{\Omega} = 0 \quad \forall f, \, g \in L^2(\Omega). \tag{3.55}$$

We propose a quadrature rule of the form:

$$\int_\Omega f\,dV \approx \int_\Omega f_p\,dV + \sum_{q=1}^{N_{qp}} w_q f_n(\mathbf{x}_q), \tag{3.56}$$

where it is supposed that the projection operators Π_k^Ω and π_k^Ω are well-defined on Ω, and $\int_\Omega f_p\,dV$ may be computed exactly using the methodology proposed by Chin et al. in [12]. Furthermore, if we wish to integrate the product fg where $f,\, g \in L^2(\Omega)$, we may write

$$\int_\Omega fg\,dV = \langle f, g\rangle_\Omega = \langle \Pi_k^\Omega f + \pi_k^\Omega f, \Pi_k^\Omega g + \pi_k^\Omega g\rangle_\Omega, \tag{3.57}$$

which, by the linearity of the $L^2(\Omega)$ inner product, and by the orthogonality of $\Pi_k^\Omega f$ and $\pi_k^\Omega g$ (and of $\pi_k^\Omega f$ and $\Pi_k^\Omega g$), yields

$$\int_\Omega fg\,dV = \langle \Pi_k^\Omega f, \Pi_k^\Omega g\rangle_\Omega + \langle \pi_k^\Omega f, \pi_k^\Omega g\rangle_\Omega, \tag{3.58}$$

and thus

$$\int_\Omega fg\,dV \approx \int_\Omega f_p g_p\,dV + \sum_{q=1}^{N_{qp}} w_q f_n(\mathbf{x}_q) g_n(\mathbf{x}_q). \tag{3.59}$$

This is effectively equivalent to integrating the product of all low-order polynomials exactly, while integrating the product of all non-polynomial "remainders" approximately, using a quadrature rule.

If we are only given evaluations of a function f at a set of discrete (quadrature) points $\{\mathbf{x}_q\}_{q=1}^{N_{qp}}$, then we must construct a low-order polynomial projection operator by considering the least-squares problem:

$$\min_{f_p \in P^k(\Omega)} \frac{1}{2} ||f_p - f||_\Omega^2, \tag{3.60}$$

where $||f||_\Omega = \sqrt{\langle f, f\rangle_\Omega}$ is deliberately approximated using the element's quadrature rule:

$$\langle f, f\rangle_\Omega \approx \sum_{q=1}^{N_{qp}} w_q \left[f(\mathbf{x}_q)\right]^2. \tag{3.61}$$

For a given polynomial basis $\{z_a\}_{a=1}^K$ which spans $P^k(\Omega)$, we may write

$$f_p(\mathbf{x}) = \sum_{a=1}^{K} z_a(\mathbf{x}) c_a = \mathbf{z}^T(\mathbf{x})\,\mathbf{c}, \tag{3.62}$$

and the solution to (3.61) satisfies

$$\sum_{a=1}^{K}\sum_{q=1}^{N_{qp}} w_q z_b(\mathbf{x}_q) z_a(\mathbf{x}_q) c_a = \sum_{q=1}^{N_{qp}} w_q z_b(\mathbf{x}_q) f(\mathbf{x}_q) \quad \forall b = 1, \ldots, K, \tag{3.63}$$

The above may be written in matrix-vector format as $\mathbf{Z}^T\mathbf{W}\mathbf{Z}\mathbf{c} = \mathbf{Z}^T\mathbf{W}\mathbf{f}$, where we denote $f_i = f(\mathbf{x}_i)$, $W_{ii} = w_i$, $W_{ij} = 0\,\forall i \neq j$, and $Z_{ij} = z_j(\mathbf{x}_i)$. The discrete polynomial projection operator $\mathbf{\Pi}_k^\Omega : \mathbb{R}^{N_{qp}} \mapsto \mathbb{R}^K$ is computed as $\mathbf{\Pi}_k^\Omega = (\mathbf{Z}^T\mathbf{W}\mathbf{Z})^{-1}\mathbf{Z}^T\mathbf{W}$, and the complement operator $\boldsymbol{\pi}_k^\Omega : \mathbb{R}^{N_{qp}} \mapsto \mathbb{R}^{N_{qp}}$ is $\boldsymbol{\pi}_k^\Omega = \mathbf{1}_{N_{qp}} - \mathbf{Z}\mathbf{\Pi}_k^\Omega$. Consequently,

$$\langle \Pi_k^\Omega f, \Pi_k^\Omega g\rangle_\Omega = \langle \mathbf{z}^T\mathbf{\Pi}_k^\Omega\mathbf{f}, \mathbf{z}^T\mathbf{\Pi}_k^\Omega\mathbf{g}\rangle_\Omega = \mathbf{f}^T\left[\mathbf{\Pi}_k^{\Omega^T}\left(\int_\Omega \mathbf{z}\otimes\mathbf{z}\,dV\right)\mathbf{\Pi}_k^\Omega\right]\mathbf{g}, \tag{3.64}$$

$$\langle \pi_k^\Omega f, \pi_k^\Omega g\rangle_\Omega \approx \sum_{q=1}^{N_{qp}} w_q f_n(\mathbf{x}_q) g_n(\mathbf{x}_q) = \mathbf{f}^T\left[\boldsymbol{\pi}_k^{\Omega^T}\mathbf{W}\boldsymbol{\pi}_k^\Omega\right]\mathbf{g}, \tag{3.65}$$

and thus

$$\int_\Omega fg\,dV \approx \mathbf{f}^T\mathbf{M}_k\mathbf{g} = \sum_{q=1}^{N_{qp}}\sum_{p=1}^{N_{qp}} M_k(\mathbf{x}_q,\mathbf{x}_p)\, f(\mathbf{x}_q)\, g(\mathbf{x}_p), \tag{3.66}$$

$$\mathbf{M}_k \equiv \left[\mathbf{\Pi}_k^{\Omega^T}\left(\int_\Omega \mathbf{z}\otimes\mathbf{z}\,dV\right)\mathbf{\Pi}_k^\Omega\right] + \left[\boldsymbol{\pi}_k^{\Omega^T}\mathbf{W}\boldsymbol{\pi}_k^\Omega\right]. \tag{3.67}$$

We shall refer to this form of integration as *selective modal quadrature*, given that the products of particular low-order polynomial modes are integrated exactly, and the products of any higher-order modes are approximated using the element's quadrature rules. The advantage of modal quadrature is that we may exactly integrate any terms which directly impact quadrature consistency. Consequently, nearly any stable numerical integration scheme (e.g. composite mid-point quadrature) may be used to integrate the higher-order products.

Rather than storing the independent quadrature weights $w_q = w(\mathbf{x}_q)$, selective modal quadrature requires the storage of a generalized quadrature weighting matrix $M_k(\mathbf{x}_q, \mathbf{x}_p)$. Alternatively, for the sake of efficiency, if the function g is known a priori (e.g. if g is a test function for a weighted residual method), then we need only store the "augmented" test function values:

$$\tilde{g}^{(k)}(\mathbf{x}_q) = \sum_{p=1}^{N_{qp}} \frac{M_k(\mathbf{x}_q,\mathbf{x}_p)}{w_q}\, g(\mathbf{x}_p), \tag{3.68}$$

and all integrals involving f and g may be carried out via

$$\int_{\Omega} f g \, dV \approx \sum_{q=1}^{N_{qp}} w_q \, \tilde{g}^{(k)}(\mathbf{x}_q) \, f(\mathbf{x}_q). \tag{3.69}$$

If applied to the stress divergence integral appearing in (2.39), the resulting expression would resemble a gradient correction scheme in some respects, although it should be noted that the above procedure would need to be applied separately to each term appearing in the weak form (including boundary integrals). Specifically, the corresponding integration of the residual equations in (2.39) would be carried out via

$$\int_{\mathcal{B}_0} P_{ij} \phi_{a,j} \, dV \approx \sum_{q=1}^{N_{qp}} w_q P_{ij}(\mathbf{x}_q) \tilde{\phi}_{a,j}^{(k)}(\mathbf{x}_q), \tag{3.70}$$

$$\int_{\mathcal{B}_0} \rho_0 b_i \phi_a \, dV \approx \sum_{q=1}^{N_{qp}} w_q \rho_0(\mathbf{x}_q) b_i(\mathbf{x}_q) \tilde{\phi}_a^{(k-1)}(\mathbf{x}_q), \tag{3.71}$$

$$\int_{\Gamma_0^N} \bar{p}_i \phi_a \, dA \approx \sum_{b=1}^{N_{bp}} w_b \bar{p}_i(\mathbf{x}_b) \tilde{\phi}_a^{(k)}(\mathbf{x}_b), \tag{3.72}$$

where $\tilde{\phi}_a^{(k)}$ and $\tilde{\phi}_{a,j}^{(k)}$ denote the "augmented" test functions are their corresponding gradients, and k is the indicated order of quadrature consistency (required to pass patch tests up to order $k+1$).

References

[1] D. N. Arnold, D. Boffi, and R. S. Falk. Approximation by quadrilateral finite elements. *Mathematics of Computation*, 71(239):909–922, 2002.

[2] D. N. Arnold, D. Boffi, R. S. Falk, and L. Gastaldi. Finite element approximation on quadrilateral meshes. *Communications in Numerical Methods in Engineering*, 17(11):805–812, 2001.

[3] Ivo Babuška. Error-bounds for finite element method. *Numerische Mathematik*, 16:322–333, 1971.

[4] Ivo Babuška and Manil Suri. Locking effects in the finite element approximation of elasticity problems. *Numerische Mathematik*, 62:439–463, 1992.

[5] Ivo Babuška and Manil Suri. On locking and robustness in the finite element method. *SIAM Journal on Numerical Analysis*, 29(5):1261–1293, 1992.

[6] F. Bassi, L. Botti, A. Colombo, D.A. Di Pietro, and P. Tesini. On the flexibility of agglomeration based physical space discontinuous galerkin discretizations. *Journal of Computational Physics*, 231(1):45 – 65, 2012.

[7] J. E. Bishop. A displacement-based finite element formulation for general polyhedra using harmonic shape functions. *International Journal for Numerical Methods in Engineering*, 97:1–31, 2014.

[8] Franco Brezzi. On the existence, uniqueness and approximation of saddle-point problems arising from lagrangian multipliers. *ESAIM: Mathematical Modelling and Numerical Analysis - Modlisation Mathmatique et Analyse Numrique*, 8:129–151, 1974.

[9] Jiun-Shyan Chen, Michael Hillman, and Marcus Rüter. An arbitrary order variationally consistent integration for galerkin meshfree methods. *International Journal for Numerical Methods in Engineering*, 95:387–418, 2013.

[10] H. Chi, L. Beirão da Veiga, and G. H. Paulino. Some basic formulations of the virtual element method (vem) for finite deformations. *Computer Methods in Applied Mechanics and Engineering*, 318:148–192, 2017.

[11] Heng Chi, Cameron Talischi, Oscar Lopez-Pamies, and Glaucio H. Paulino. A paradigm for higher-order polygonal elements in finite elasticity using a gradient correction scheme. *Computer Methods in Applied Mechanics and Engineering*, 306:216–251, 2016.

[12] Eric B. Chin, Jean B. Lasserre, and N. Sukumar. Numerical integration of homogeneous functions on convex and nonconvex polygons and polyhedra. *Computational Mechanics*, 56:967–981, 2015.

[13] Zhong ci Shi. The f-e-m-test for convergence of nonconforming finite elements. *Mathematics of Computation*, 49(180):391–405, 1987.

[14] M. Cicuttin, D.A. Di Pietro, and A. Ern. Implementation of discontinuous skeletal methods on arbitrary-dimensional, polytopal meshes using generic programming. *Journal of Computational and Applied Mathematics*, 2017.

[15] L. Beirão da Veiga, F. Brezzi, A. Cangiani, G. Manzini, L. D. Marini, and A. Russo. Basic principles of virtual element methods. *Computer Methods in Applied Mechanics and Engineering*, 23:199–214, 2013.

[16] L. Beirão da Veiga, C. Lovadina, and D. Mora. A virtual element method for elastic and inelastic problems on polytope meshes. *Computer Methods in Applied Mechanics and Engineering*, 295:327–346, 2015.

[17] E. A. de Souza Neto, D. Perić, M. Dukto, and D. R. J. Owen. Design of simple low order finite elements for large strain analysis of nearly incompressible solids. *International Journal of Solids and Structures*, 33:3277–3296, 1996.

[18] C. R. Dohrmann and M. M. Rashid. Polynomial approximation of shape function gradients from element geometries. *International Journal for Numerical Methods in Engineering*, 53:945–958, 2002.

[19] D. A. Dunavant. High degree efficient symmetrical gaussian quadrature rules for the triangle. *International Journal for Numerical Methods in Engineering*, 21(6):1129–1148, 1985.

[20] Mohamed S. Ebeida and Scott A. Mitchell. Uniform random voronoi meshes. *Proceedings of the 20th International Meshing Roundtable*, pages 273–290, 2011.

[21] Mohamed Salah Ebeida. Vorocrust v. 1.0, Jul 2017.

[22] Carlos A. Felippa. *Introduction to Finite Element Methods*. University of Colorado, Boulder, 2004.

[23] D. P. Flanagan and T. Belytschko. A uniform strain hexahedron and quadrilateral with orthogonal hourglass control. *International Journal for Numerical Methods in Engineering*, 17:679–706, 1981.

[24] Michael S. Floater. Mean value coordinates. *Computer Aided Geometric Design*, 20:19–27, 2003.

[25] Arun Gain, Cameron Talischi, and Glaucio H. Paulino. On the virtual element method for three-dimensional elasticity problems on arbitrary polyhedral meshes. *Computer Methods in Applied Mechanics and Engineering*, 282, 11 2013.

[26] Xifeng Gao, Wenzel Jakob, Marco Tarini, and Daniele Panozzo. Robust hex-dominant mesh generation using field-guided polyhedral agglomeration. *ACM Transactions on Graphics*, 36, 2017.

[27] William J. Gordon and James A. Wixom. Pseudo-harmonic interpolation on convex domains. *SIAM Journal on Numerical Analysis*, 11(5):909–933, 1974.

[28] Axel Grundmann and H. M. Möller. Invariant integration formulas for the n-simplex by combinatorial methods. *SIAM Journal on Numerical Analysis*, 15(2):282–290, 1978.

[29] Jan S. Hesthaven and Tim Warburton. *Nodal Discontinuous Galerkin Methods: Algorithms, Analysis, and Applications*. Springer Publishing Company, Incorporated, 1st edition, 2010.

[30] Thomas J. R. Hughes. *The Finite Element Method–Linear Static and Dynamic Finite Element Analysis*. Dover Publications, 2000.

[31] Pushkar Joshi, Mark Meyer, Tony DeRose, Brian Green, and Tom Sanocki. Harmonic coordinates for character articulation. *ACM Transactions on Graphics*, 26, 2007.

[32] Mika Juntunen and Rolf Stenberg. Nitsche's method for general boundary conditions. *Mechanics of Computation*, 78(267):1353–1374, 2009.

[33] Nam-Sua Lee and Klaus-Jürgen Bathe. Effects of element distortions on the performance of isoparametric elements. *International Journal for Numerical Methods in Engineering*, 36:3553–3576, 1993.

[34] Qiaoluan H. Li and Junping Wang. Weak galerkin finite element methods for parabolic equations. *Numerical Methods for Partial Differential Equations*, 29:2004–2024, 2013.

[35] Guang Lin, Jiangguo Liu, and Farrah Sadre-Marandi. A comparative study on the weak galerkin, discontinuous galerkin, and mixed finite element methods. *Journal of Computational and Applied Mathematics*, 273:346–362, 2015.

[36] Richard H. MacNeal. A theorem regarding the locking of tapered four-noded membrane elements. *International Journal for Numerical Methods in Engineering*, 24:1793–1799, 1987.

[37] Sebastian Martin, Peter Kaufmann, Mario Botsch, Martin Wicke, and Markus Gross. Polyhedral finite elements using harmonic basis functions. *Eurographics Symposium on Geometry Processing 2008*, 27(5), 2008.

[38] L. Mu, J. Wang, and Y. Wang. A computational study of the weak galerkin method for second-order elliptic equations. *Numerical Algorithms*, 63:753, 2013.

[39] L. Mu, J. Wang, and X. Ye. Weak galerkin finite element method for second-order elliptic problems on polytopal meshes. *International Journal of Numerical Analysis and Modeling*, 12:31–53, 2015.

[40] Lin Mu, Junping Wang, and Xiu Ye. A weak galerkin finite element method with polynomial reduction. *Journal of Computational and Applied Mathematics*, 285:45–58, 2015.

[41] Daniel Pantuso and Klaus-Jürgen Bathe. On the stability of mixed finite elements in large strain analysis of incompressible solids. *Finite Elements in Analysis and Design*, 28:83–104, 1997.

[42] M. M. Rashid. Incremental kinematics for finite element applications. *International Journal for Numerical Methods in Engineering*, 36:3937–3956, 1993.

[43] M. M. Rashid and P. M. Gullett. On a finite element method with variable element topology. *Computer Methods in Applied Mechanics and Engineering*, 190:1509–1527, 2000.

[44] M. M. Rashid and A. Sadri. The partitioned element method in computational solid mechanics. *Computer Methods in Applied Mechanics and Engineering*, 237–240:152–165, 2012.

[45] M. M. Rashid and M. Selimotić. A three-dimensional finite element method with arbitrary polyhedral elements. *International Journal for Numerical Methods in Engineering*, 67:226–252, 2006.

[46] J.-F. Remacle, J. Lambrechts, B. Seny, E. Marchandise, A. Johnen, and C. Geuzainet. Blossom-quad: a non-uniform quadrilateral mesh generator using a minimum cost perfect matching algorithm. *International Journal for Numerical Methods in Engineering*, 89:1102–1119, 2012.

[47] Béatrice Rivière. *Discontinuous Galerkin Methods for Solving Elliptic and Parabolic Equations: Theory and Implementation*. Society for Industrial and Applied Mathematics, 3600 Market Street, 6th Floor, Philadelphia, PA 19104-2688 USA, 2008.

[48] Mili Selimotić. *Polyhedral Finite-Element Approximants in 3D Solid Mechanics*. PhD thesis, University of California, Davis, 2008.

[49] J. C. Simo and F. Armero. Geometrically non-linear enhanced strain mixed methods and the method of incompatible modes. *International Journal for Numerical Methods in Engineering*, 33:1413–1449, 1992.

[50] J. C. Simo, F. Armero, and R. L. Taylor. Improved versions of assumed enhanced strain tri-linear elements for 3d finite deformation problems. *Computer Methods in Applied Mechanics and Engineering*, 110:359–386, 1993.

[51] J. C. Simo and M. S. Rifai. A class of mixed assumed strain methods and the method of incompatible modes. *International Journal for Numerical Methods in Engineering*, 29:1595–1638, 1990.

[52] Friedrich Stummel. The generalized patch test. *SIAM Journal on Numerical Analysis*, 16(3):449–471, 1979.

[53] Friedrich Stummel. The limitations of the patch test. *International Journal for Numerical Methods in Engineering*, 16:177–188, 1980.

[54] N. Sukumar. Construction of polygonal interpolants: a maximum entropy approach. *International Journal for Numerical Methods in Engineering*, 61:2159–2181, 2004.

[55] Manil Suri. On the robustness of the h- and p-versions of the finite-element method. *Journal of Computational and Applied Mathematics*, 35:303–310, 1991.

[56] Theodore Sussman and Klaus-Jürgen Bathe. Spurious modes in geometrically nonlinear small displacement finite elements with incompatible modes. *Computers & Structures*, 140:14–22, 2014.

[57] Cameron Talischi and Glaucio H. Paulino. Addressing integration error for polygonal finite elements through polynomial projections: A patch test connection. *Mathematical Models and Methods in Applied Sciences*, 24:1701–1727, 2014.

[58] Cameron Talischi, Glaucio H. Paulino, Anderson Pereira, and Ivan F. M. Menezes. Polymesher: a general-purpose mesh generator for polygonal elements written in matlab. *Structural and Multidisciplinary Optimization*, 45(3):309–328, Mar 2012.

[59] Cameron Talischi, Anderson Pereira, Ivan F. M. Menezes, and Glaucio H. Paulino. Gradient correction for polygonal and polyhedral finite elements. *International Journal for Numerical Methods in Engineering*, 102:728–747, 2015.

[60] R. L. Taylor, J. C. Simo, O. C. Zienkiewicz, and A. C. H. Chan. The patch testa condition for assessing fem convergence. *International Journal for Numerical Methods in Engineering*, 22(1):39–62, 1986.

[61] Eugene L. Wachspress. *A Rational Finite Element Basis*. Academic Press, 1975.

[62] J. Wang and X. Ye. A weak galerkin finite element method for second-order elliptic problems. *Journal of Computational and Applied Mathematics*, 241:103–115, 2013.

[63] X. Wang, N.S. Malluwawadu, F. Gao, and T.C. McMillan. A modified weak galerkin finite element method. *Journal of Computational and Applied Mathematics*, 271:319–329, 2014.

[64] Wikiversity. Introduction to elasticity/plate with hole in tension, 2017.

[65] Robert Winkler. Comments on membrane locking. *Proceedings in Applied Mathematics and Mechanics*, 10:229–230, 2010.